An axisymmetric extended plane strain model for systems codes of the toroidal field coil of a tokamak at the inboard midplane [R08]

R01 date 2021/08/17
R08 date 2022/02/14

Dr. Charles PS Swanson [*], Dr. Sebastien Kahn[†]

1 Abstract

The toroidal field (TF) coil of a tokamak magnetic fusion reactor will experience significant steady-state structural loads due to the Lorentz force. The ability to predict these loads is essential for the design and analysis of such reactors. While a fully 3D Finite Element Analysis (FEA) is required to validate a detailed design, a 0D system design code ony requires an approximately correct answer. These systems codes are meant to rapidly iterate through the space of possible designs, rather than produce highly accurate results of a single design. Here, we present a simple model of the stresses and strains within the TF coil at the inboard midplane of the tokamak, resolved in the radial direction. No out-of-plane forces from the poloidal field are considered. This model assumes axisymmetry and symmetry (long) in the axial direction. The TF coil is assumed to be constructed of any number of layers, within which materials properties are uniform. The 1D radially-resolved problem is reduced to a 0D calculation with the use of a Green's Function solution to Lamé cylindrical stress equations incorporating a general body force in the radial direction. Poisson's Ratio effects are included. Boundary conditions between layers are reduced to matrix multiplication. Boundary conditions at the inboard and outboard side are likewise reduced to a single 3×3 matrix inversion or Gaussian elimination. The axial force (tension) is assumed to be known. The axial strain is assumed to be constant (an "extended plane strain problem") and is found as a result of the matrix inversion. Transverse-isotropic materials can be considered. The

[*] cswanson@pppl.gov
[†] sebastien.kahn@ukaea.uk

inner boundary condition can assume either a finite-radius open bore, or a plugged bore ($r_{bore} = 0$). An inner set of layers may be assumed to be frictionally decoupled from the outer layers, in that they may be considered to carry no axial force.

2 Introduction

The toroidal field (TF) coils of a tokamak will experience significant steady-state structural loads. This is due to the high magnetic fields required of these devices, which at the high end could reach above 25 Tesla,[1] corresponding to a magnetic pressure of > 200 MPa. Clearly, it is essential to predict and understand these magnetic loads.

The internal stresses and strains in the TF coil can be computed to very high accuracy using Finite Element Analysis (FEA) tools such as Ansys and COMSOL. However, before a tokamak design reaches the level of detail that requires FEA, it must first be arrived-at by approximate methods. The codes that use these approximate methods to evaluate and iterate over a large number of design points are called systems codes. There are many such codes in the literature, such as CCFE's PROCESS,[2, 3] Tokamak Energy's TESC,[4, 5] General Atomics's GASC,[6, 7] and ORNL's Unnamed FESS Systems code.[8, 9] For a very tutorial approach, see papers from J. Freidberg's group.[10, 11, 12]

Systems codes require approximate models, as they must run quickly but capture the essential interaction between the major systems of the tokamak. Because of this, explicit analyses are preferred over implicit. FEA takes too long. Some examples of very simple TF coil load models include: The magnetic virial theorem (distinct from the magnetic *plasma* virial theorem) which relates the mass of structural material to the stored magnetic energy,[13] and lumped-sum TF coil models.[10]

We present a more sophisticated model which radially resolves the stress and strain distribution within any number of layers. We consider the inboard midplane of the TF coil, as this is likely representative of the highest stresses in the coil. We assume that all materials are elastic. We assume that the behavior in the inboard midplane is the same of that of the same plane, projected infinitely into the axial direction ($\partial_z = 0$). See Figure 1. Assuming the geometry and materials properties do not change with the axial coordinate is called the "generalized plane strain problem."[14] We neglect any shear, making this the further simplified "extended plane strain problem," in which axial strain is constant. We assume the problem is axisymmetric ($\partial_\theta = 0$). We assume that there is some prescribed axial force/tension, but that all volumetric force density (body force) is in the radial direction. Finally, we assume that the material is isotropic or transverse-isotropic.

The solution to this model progresses in the following way:

- Section 3: The relationships between stress, strain, and displacement are established (the Lamé thick cylinder equations)
- Section 4: A solution to these equations is found assuming that materials properties are uniform and there is no body force

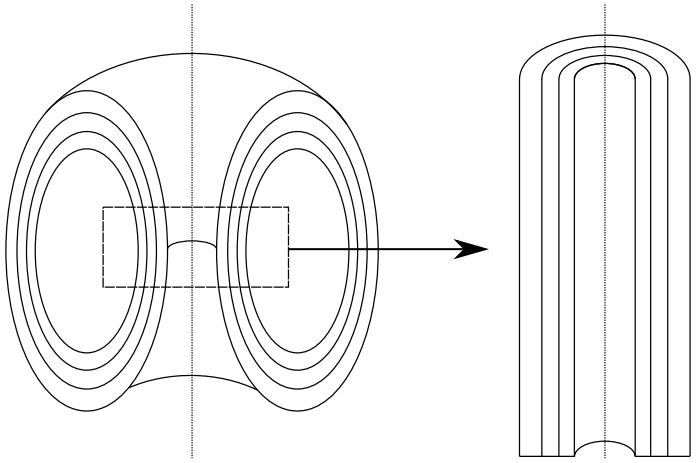

Figure 1: The assumed geometry of our problem: The materials properties, geometry, and stresses/strains at the inboard midplane of the TF coil are assumed to be uniform in the axial direction and axisymmetric.

- Section 5: A Green's function approach generalizes the uniform-layer solution to include fully general radial body forces
- Section 6: Boundary conditions between layers of uniform material properites are specified
- Section 7: The solution for all radii is posed in terms of two degrees of freedom related to the outermost edge and the axial strain
- Section 8: The axial force / tension of this solution is found
- Section 9: Boundary conditions at the inner and outer surface are written, as is the condition that the axial force/tension is known
- Section 10 The solution to these boundary conditions is produced via a single 3×3 matrix inversion or Gaussian elimination

Additional items are discussed:

- Section 11: The model is generalized from isotropic to transverse-isotropic materials
- Section 12: The functional form of $f(r)$, the radial force density profile, is discussed, and analytic forms of relative integrals are given.
- Section 13: Computing bulk, effective materials properties from small-scale mixtures of heterogeneous materials is discussed. This is called the "smearing" of materials properties, and is used to compute, for example, materials properties of axial filaments embedded in a bulk matrix.
- Section 14: The model is extended to allow that an inner section of layers do not contribute to the axial force F_z, as though a central solenoid has been frictionally decoupled from the TF while being bucked and wedged.

- Section 15: A MATLAB script is given which implements the model

The present algorithm incorporates and extends an algorithm by S. Kahn for the PROCESS code.[15, 16] The present algorithm uses an inner boundary condition for which the plugged case is the limiting behavior of the open-bore case for $r_{bore} \to 0$. The present algorithm requires a much smaller matrix inversion / Gaussian elimination, 3×3 for any number of layers, as opposed to the prior algorithm's $2N \times 2N$ where N is the number of layers. This algorithm therefore takes $O(N)$ compute time rather than $O(N^3)$, making it more applicable to many-layered or graded coils. The present model leaves the dependence on the radial body force as a fully general $f(r)$ integral, allowing specialization to the prior model's Lorentz force or considering general forces.

This model does not consider out-of-plane forces produced on the TF coil by the poloidal field (PF) coils. These forces are now known to be significant.

3 Stress, strain, and displacement

In cylindrical coordinates, the normal strains $\epsilon_q \equiv \epsilon_{qq}$ have the following relationship to the axisymmetric displacement $\vec{u} = u_r \hat{r} + u_z \hat{z}$:

$$\epsilon_r = \partial_r u_r \tag{1}$$

$$\epsilon_\theta = \frac{1}{r} u_r \tag{2}$$

$$\epsilon_z = \partial_z u_z \tag{3}$$

The following sections will consider the simpler case of isotropic materials. For the more complex transverse-isotropic case, see Section 11

The strains are computed from the normal stresses $\sigma_q \equiv \sigma_{qq}$ using the compliance form of Hooke's Law, which for an isotropic material is:

$$\epsilon_r = \frac{1}{E}(\sigma_r - \nu(\sigma_\theta + \sigma_z)) \tag{4}$$

$$\epsilon_\theta = \frac{1}{E}(\sigma_\theta - \nu(\sigma_r + \sigma_z)) \tag{5}$$

$$\epsilon_z = \frac{1}{E}(\sigma_z - \nu(\sigma_r + \sigma_\theta)) \tag{6}$$

where E is the Young's modulus and ν is the Poisson's ratio of the material. Likely values of E are in the tens to hundreds of gigapascals ($10^{10} - 10^{11}$ GPa). Values of ν are between 0 and 1/2, often around $\nu \sim 0.3$.

These equations can be inverted into the stiffness form of Hooke's Law:

$$\sigma_r = \bar{E}(\epsilon_r + \bar{\nu}(\epsilon_\theta + \epsilon_z)) \tag{7}$$

$$\sigma_\theta = \bar{E}(\epsilon_\theta + \bar{\nu}(\epsilon_r + \epsilon_z)) \tag{8}$$

$$\sigma_z = \bar{E}(\epsilon_z + \bar{\nu}(\epsilon_r + \epsilon_\theta)) \tag{9}$$

where $\bar{E}$ and $\bar{\nu}$ are the effective Young's modulus and Poisson's ratio holding *strain* rather than *stress* cross-terms constant [EDIT: Do these have names?]:

$$\bar{E} \equiv E\frac{1-\nu}{1-\nu-2\nu^2} \tag{10}$$

$$\bar{\nu} \equiv \frac{\nu}{1-\nu} \tag{11}$$

Finally, these quantities may be related to each other via a force balance equilibrium on a differential volume $dV = r \times dr \times d\theta \times dz$:

$$\partial_V F_r = 0 = f - \partial_r \sigma_r - \frac{1}{r}\sigma_r + \frac{1}{r}\sigma_\theta \tag{12}$$

where f is the volumetric force density in the radial direction, also called "body force," for example the Lorentz force $(\vec{j} \times \vec{B}) \cdot \hat{r}$.

4 Uniform-layer, no-body-force solution

If $\bar{E}$ and $\bar{\nu}$ are constant, we are considering a layer of uniform material. The equilibrium equation Equation 12 is therefore simplified, and plugging in the stresses (Equations 7 and 8) then the strains (Equations 1 and 2) gives:

$$0 = \frac{1}{\bar{E}}f - \partial_r^2 u - \frac{1}{r}\partial_r u + \frac{1}{r^2}u \tag{13}$$

If $f = 0$ we are considering the case that this layer has no body force.

$$0 = -\partial_r^2 u - \frac{1}{r}\partial_r u + \frac{1}{r^2}u \tag{14}$$

where $u \equiv u_r$, the only displacement we are worried about.

The solution to this equation has the form

$$u(r) = Ar + B\frac{1}{r} \tag{15}$$

where A, B are free parameters to be determined by boundary conditions, the so-called Lamé parameters. This solution can be plugged into Equations 7, 8, 1, and 2 to give the radial and azimuthal stress:

$$\sigma_r(r) = \bar{E}[A(1+\bar{\nu}) - B(1-\bar{\nu})\frac{1}{r^2} + \bar{\nu}\epsilon_z] \tag{16}$$

$$\sigma_\theta(r) = \bar{E}[A(1+\bar{\nu}) + B(1-\bar{\nu})\frac{1}{r^2} + \bar{\nu}\epsilon_z] \tag{17}$$

In engineering circles, these equations are also used to model thick cylindrical pressure vessels, where they are called the Lamé cylindrical stress equations. They are used with the boundary condition that $\sigma_r(r_{in})$ is equal to the pressure on the inside of the vessel P_{in}, and that $\sigma_r(r_{out})$ is equal to the pressure on the inside of the vessel P_{out}.

Note also that the plugged case, with $r_{in} = 0$, has the boundary condition that $u(0) = 0$, the radial displacement at the origin is zero. Plugging this into Equation 15, we get that $B = 0$. Plugging this into Equations 16 and 17, we get that $\sigma_r = \sigma_\theta = P_{out}$ is constant, the expected hydrostatic-like case.

5 Body forces within layers

If the uniform layer under consideration is allowed to experience a general radial body force $f(r)$, Equation 13 once again applies rather than Equation 14. The former is reproduced here:

$$0 = \frac{1}{\bar{E}}f - \partial_r^2 u - \frac{1}{r}\partial_r u + \frac{1}{r^2}u$$

Note that this is an equation with homogeneous and inhomogeneous terms, and is therefore susceptible to a Green's Function approach. The result is that, rather than being constant within the layers, $A(r)$ and $B(r)$ will be functions of r:

$$A(r) = A^{out} - \frac{1}{2\bar{E}}\int_r^{r_{out}} dr \times f(r) \tag{18}$$

$$B(r) = B^{out} + \frac{1}{2\bar{E}}\int_r^{r_{out}} dr \times r^2 f(r) \tag{19}$$

where $A^{out} \equiv A(r_{out})$ and $B^{out} \equiv B(r_{out})$. For the body forces of interest, these integrals are analytically solvable. Two useful cases, that of a uniform force and a Lorentz force caused by current density, are given in Section 12.

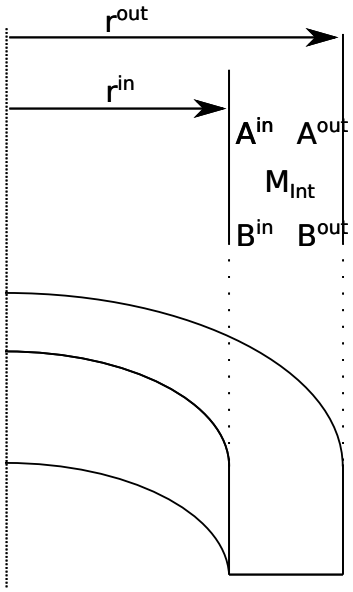

Figure 2: For a uniform layer that has inner radius r_{in} and outer radius r_{out}, A^{in}, B^{in} are the Lamé parameters (see Equation 15) at the inner radius and A^{out}, B^{out} are the Lamé parameters at the outer radius. The matrix M_{Int} transforms the outer parameters into the inner parameters.

One might expect the functional forms of σ_r and σ_θ to disagree with the form found for a force-free layer, Equations 16 and 17 because of the $\partial_r A, \partial_r B$ terms that now exist in $\partial_r u$. However, these terms cancel and Equations 16 and 17 are fortuitously still true with A, B replaced with $A(r), B(r)$:

$$\sigma_r(r) = \bar{E}[A(r)(1+\bar{\nu}) - B(r)(1-\bar{\nu})\frac{1}{r^2} + \bar{\nu}\epsilon_z] \tag{20}$$

$$\sigma_\theta(r) = \bar{E}[A(r)(1+\bar{\nu}) + B(r)(1-\bar{\nu})\frac{1}{r^2} + \bar{\nu}\epsilon_z] \tag{21}$$

As we will see in Section 6, it will become extremely useful to define a matrix which transforms the outer Lamé parameters into the inner ones. To cast Equations 18 and 19 into a matrix that relates these two sets of parameters, we require so-called augmented or homogeneous coordinates, as is commonly used in Affine transformations:

$$\begin{pmatrix} A^{in} \\ B^{in} \\ 1 \end{pmatrix} = \begin{bmatrix} 1 & 0 & -\frac{1}{2\bar{E}}\int_{r_{in}}^{r_{out}} dr \times f(r) \\ 0 & 1 & \frac{1}{2\bar{E}}\int_{r_{in}}^{r_{out}} dr \times r^2 f(r) \\ 0 & 0 & 1 \end{bmatrix} \begin{pmatrix} A^{out} \\ B^{out} \\ 1 \end{pmatrix} \tag{22}$$

However, as we will see in Section 10, the matrix will serve us best if the solution vector is actually actually augmented by *two* additional coordinates, one of which is the constant uniform

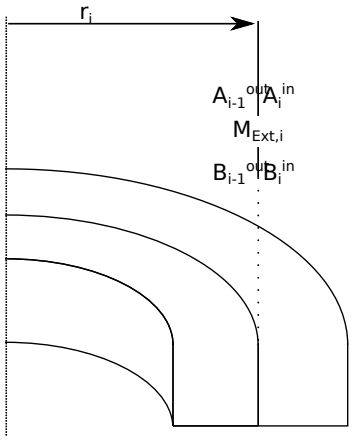

Figure 3: For two uniform layers, layer $i-1$ and layer i separated by radius r_i, boundary conditions relate the Lamé parameters at the outer edge of layer $i-1$ to those at the inner edge of layer i. The matrix $M_{Ext,i}$ transforms the inner parameters of layer i into the outer parameters of layer $i-1$.

axial strain ϵ_z:

$$\begin{pmatrix} A^{in} \\ B^{in} \\ \epsilon_z \\ 1 \end{pmatrix} = M_{Int} \begin{pmatrix} A^{out} \\ B^{out} \\ \epsilon_z \\ 1 \end{pmatrix} = \begin{bmatrix} 1 & 0 & 0 & -\frac{1}{2\bar{E}} \int_{r_{in}}^{r_{out}} dr \times f(r) \\ 0 & 1 & 0 & \frac{1}{2\bar{E}} \int_{r_{in}}^{r_{out}} dr \times r^2 f(r) \\ 0 & 0 & 1 & 0 \\ 0 & 0 & 0 & 1 \end{bmatrix} \begin{pmatrix} A^{out} \\ B^{out} \\ \epsilon_z \\ 1 \end{pmatrix} \tag{23}$$

Where here we have defined the matrix M_{Int} as the "internal transformation matrix," the matrix that transforms the Lamé parameters at the outer edge of the layer into those parameters at the inner edge of the layer.

6 Boundary conditions between layers

Suppose layer i is that layer which exists between radii r_i and r_{i+1}.

The boundary conditions between two layers are:

$$u_{i-1}(r_i) = u_i(r_i) \tag{24}$$

continuity of displacement and

$$\sigma_{r,i-1}(r_i) = \sigma_{r,i}(r_i) \tag{25}$$

continuity of radial stress.

Expanding these boundary conditions, they become

$$A_{i-1}^{out} r_i + B_{i-1}^{out} \frac{1}{r_i} = A_i^{in} r_i + B_i^{in} \frac{1}{r_i} \tag{26}$$

and

$$\bar{E}_{i-1}[A_{i-1}^{out}(1+\bar{\nu}_{i-1}) - B_{i-1}^{out}(1-\bar{\nu}_{i-1})\frac{1}{r_i^2} + \bar{\nu}_{i-1}\epsilon_z] = \bar{E}_i[A_i^{in}(1+\bar{\nu}_i) - B_i^{in}(1-\bar{\nu}_i)\frac{1}{r_i^2} + \bar{\nu}_i\epsilon_z] \tag{27}$$

These boundary conditions can be rearranged to provide $A_{i-1}^{out}, B_{i-1}^{out}$ in terms of A_i^{in}, B_i^{in}:

$$A_{i-1}^{out} = A_i^{in}\frac{1}{2}[\frac{\bar{E}_i}{\bar{E}_{i-1}}(1+\bar{\nu}_i)+1-\bar{\nu}_{i-1}] + B_i^{in}\frac{1}{r_i^2}\frac{1}{2}[1-\bar{\nu}_{i-1}-\frac{\bar{E}_i}{\bar{E}_{i-1}}(1-\bar{\nu}_i)] + \epsilon_z\frac{1}{2}[\frac{\bar{E}_i}{\bar{E}_{i-1}}\bar{\nu}_i - \bar{\nu}_{i-1}] \tag{28}$$

$$B_{i-1}^{out} = A_i^{in} r_i^2\big(1-\frac{1}{2}[\frac{\bar{E}_i}{\bar{E}_{i-1}}(1+\bar{\nu}_i)+1-\bar{\nu}_{i-1}]\big) + B_i^{in}\big(1-\frac{1}{2}[1-\bar{\nu}_{i-1}-\frac{\bar{E}_i}{\bar{E}_{i-1}}(1-\bar{\nu}_i)]\big) - \epsilon_z r_i^2\frac{1}{2}[\frac{\bar{E}_i}{\bar{E}_{i-1}}\bar{\nu}_i - \bar{\nu}_{i-1}] \tag{29}$$

As with M_{Int} in Section 5, we will be best served by a matrix to transform the inner parameter vector from layer i to the outer parameter vector from layer $i-1$:

$$\begin{pmatrix} A_{i-1}^{out} \\ B_{i-1}^{out} \\ \epsilon_z \\ 1 \end{pmatrix} = M_{Ext,i}\begin{pmatrix} A_i^{in} \\ B_i^{in} \\ \epsilon_z \\ 1 \end{pmatrix} = \begin{bmatrix} M_{1,1} & M_{1,2} & M_{1,3} & 0 \\ M_{2,1} & M_{2,2} & M_{2,3} & 0 \\ 0 & 0 & 1 & 0 \\ 0 & 0 & 0 & 1 \end{bmatrix}\begin{pmatrix} A_i^{in} \\ B_i^{in} \\ \epsilon_z \\ 1 \end{pmatrix} \tag{30}$$

$$M_{1,1} = \frac{1}{2}[\frac{\bar{E}_i}{\bar{E}_{i-1}}(1+\bar{\nu}_i) + 1 - \bar{\nu}_{i-1}] \tag{31}$$

$$M_{1,2} = \frac{1}{r_i^2}\frac{1}{2}[1-\bar{\nu}_{i-1} - \frac{\bar{E}_i}{\bar{E}_{i-1}}(1-\bar{\nu}_i)] \tag{32}$$

$$M_{1,3} = \frac{1}{2}[\frac{\bar{E}_i}{\bar{E}_{i-1}}\bar{\nu}_i - \bar{\nu}_{i-1}] \tag{33}$$

$$M_{2,1} = r_i^2(1 - M_{1,1}) \tag{34}$$

$$M_{2,2} = 1 - r_i^2 M_{1,2} \tag{35}$$

$$M_{2,3} = -r_i^2 M_{1,3} \tag{36}$$

Where here we have defined the matrix M_{Ext} as the "external transformation matrix," the matrix that transforms the Lamé parameters at the inner edge of the outer layer into those parameters at the outer edge of the inner layer.

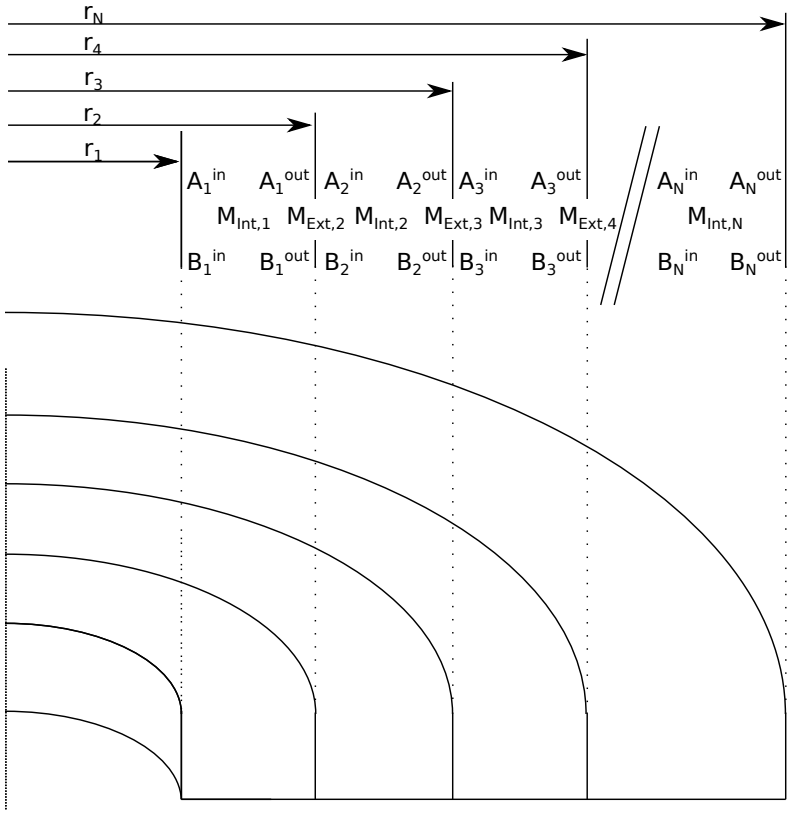

Figure 4: By multiplying successive matrices, one may produce a 4×4 matrix which transforms the outermost Lamé parameters into the Lamé parameters at any layer.

7 Specify solution for all radii if outer edge parameters are known

Let us now specify the following Lamé parameter vector notation:

$$\vec{A}_i^j = \begin{pmatrix} A_i^j \\ B_i^j \\ \epsilon_z \\ 1 \end{pmatrix} \tag{37}$$

where i is the layer index from 1 to N and j is either *in* for the innermost edge of that layer or *out* for the outermost edge of that layer.

In Section 5 we defined matrix $M_{Int,i}$ such that

$$\vec{A}_i^{in} = M_{Int,i} \vec{A}_i^{out} \tag{38}$$

In Section 6 we defined matrix $M_{Ext,i}$ such that

$$\vec{A}_{i-1}^{out} = M_{Ext,i}\vec{A}_i^{in} \tag{39}$$

By successively multiplying these matrices, one may obtain a matrix which transforms $\vec{A}_N^{out}$ into the Lamé parameter vector at any position:

$$\vec{A}_i^{in} = M_{Tot,i}\vec{A}_N^{out} = \prod_{j=i}^{N-1}[M_{Int,j}M_{Ext,j+1}]M_{Int,N}\vec{A}_N^{out} \tag{40}$$

Thus, if the Lamé parameters at the outer edge A_N^{out}, B_N^{out} are known, and the axial strain ϵ_z is known, the displacement, strain, and stress can be found at every radius. The procedure follows thus:

- Determine all internal transfer matrices $M_{Int,i}$ from the body forces $f(r)$ using Equation 23
- Determine all external transfer matrices $M_{Ext,i}$ from the stiffness form of the Young's moduli $\bar{E}$ (Equation 10), Poisson's ratios $\bar{\nu}$ (Equation 11), and the axial stress ϵ_z using Equations 30 - 36
- Determine all total transfer matrices $M_{Tot,i}$ from Equation 40
- Determine all Lamé parameter vectors from $\vec{A}_N^{out}$ and $M_{Tot,i}$ using Equation 40
- Determine radially resolved Lamé parameters $A(r), B(r)$ from Equations 18 and 19
- Determine the radially resolved displacement $u(r)$ from Equation 15, radial stress $\sigma_r(r)$ from Equation 20, and azimuthal stress σ_θ from Equation 21

All that is left is to determine the final unknown parameters, the Lamé parameters at the outer edge A_N^{out}, B_N^{out} and the axial strain ϵ_z.

8 Axial force / tension

This section computes the axial force or tension, F_z, of the solution found in Section 7. That solution has axial strain ϵ_z as an input parameter. If instead F_z is a known input parameter and ϵ_z is unknown, the matrix inversion solution in Section 10 must be used.

The axial force / tension is the areal integral of the axial stress

$$F_z = \int dA \times \sigma_z = 2\pi \int_{r_1}^{r_{N+1}} dr \times r\sigma_z(r) \tag{41}$$

As per Equation 9, this has two parts: A stiffness term proportional to $\bar{E}$ and a Poisson term proportional to $\bar{\nu}$:

$$F_z = F_{z,\bar{E}} + F_{z,\bar{\nu}} \tag{42}$$

The stiffness term is trivially calculable:

$$F_{z,\bar{E}} = \epsilon_z \int dA \times \bar{E} = \epsilon_z \langle \bar{E} A \rangle = \epsilon_z \pi \sum_{i=1}^{N} \bar{E}_i (r_{i+1}^2 - r_i^2) \tag{43}$$

The Poisson term can be fortuitously simplified via integration by parts, and is here reproduced alongside a few of the non-obvious steps:

$$F_{z,\bar{\nu}} = 2\pi \int dr \times r \bar{E} \bar{\nu} (\epsilon_r + \epsilon_\theta) = 2\pi \sum_{i=1}^{N} \bar{E}_i \bar{\nu}_i [r_{i+1} u(i+1) - r_i u(r_i)] \tag{44}$$

$$F_{z,\bar{\nu}} = 2\pi \Big[\bar{E}_N \bar{\nu}_N r_{N+1} u(r_{N+1}) - \bar{E}_1 \bar{\nu}_1 r_1 u(r_1) + \sum_{i=2}^{N} (\bar{E}_{i-1} \bar{\nu}_{i-1} - \bar{E}_i \bar{\nu}_i) r_i u(r_i) \Big] \tag{45}$$

$F_{z,\bar{\nu}}$ as a function of the outermost Lamé parameters is best expressed in inner product form:

$$\begin{aligned} F_{z,\bar{\nu}} = 2\pi \Big[& \bar{E}_N \bar{\nu}_N \begin{pmatrix} r_{N+1}^2 & 1 & 0 & 0 \end{pmatrix} \vec{A}_N^{out} - \bar{E}_1 \bar{\nu}_1 \begin{pmatrix} r_1^2 & 1 & 0 & 0 \end{pmatrix} M_{Tot,1} \vec{A}_N^{out} \\ & + \sum_{i=2}^{N} (\bar{E}_{i-1} \bar{\nu}_{i-1} - \bar{E}_i \bar{\nu}_i) \begin{pmatrix} r_i^2 & 1 & 0 & 0 \end{pmatrix} M_{Tot,i} \vec{A}_N^{out} \Big] \end{aligned} \tag{46}$$

where a row vector to the left of a column vector denotes an inner product, for example

$$\begin{pmatrix} r^2 & 1 & 0 & 0 \end{pmatrix} \vec{A} = Ar^2 + B \tag{47}$$

9 Global boundary conditions and axial force constraint

As a result of Sections 7 and 8, we now have all displacements, stresses, and strains as a function of the outermost Lamé parameters A_N^{out}, B_N^{out} and axial strain ϵ_z. We wish to know these parameters as we subject the problem to inner and outer edge boundary condition and the constraint that the axial force F_z is a known value.

9.1 Outer boundary condition

The outer edge of the outermost layer is under no radial stress:

$$\sigma_r(r_{N+1}) = 0 \tag{48}$$

This boundary condition is a condition on the outermost Lamé parameters A_N^{out}, B_N^{out} and the axial strain ϵ_z which is best expressed in inner product form:

$$\begin{pmatrix} (1+\bar{\nu}_N) r_{N+1}^2 & -1+\bar{\nu}_N & \bar{\nu}_N r_{N+1}^2 & 0 \end{pmatrix} \vec{A}_N^{out} = 0 \tag{49}$$

9.2 Inner boundary condition

There are two cases for the inner boundary condition, the plugged bore case, in which material extends all the way in to the axis of symmetry and $r_1 = 0$, and the open-bore case, in which $r_1 > 0$.

For the open-bore case, the boundary condition at the inner edge of the innermost layer is the same as the outer edge of the outermost layer, that it is under no radial stress:

$$\sigma_r(r_1) = 0 \tag{50}$$

This boundary condition can again be written as a condition on the outermost Lamé parameters A_N^{out}, B_N^{out} and the axial strain ϵ_z which is best expressed in inner product form:

$$\begin{pmatrix}(1+\bar{\nu}_1)r_1^2 & -1+\bar{\nu}_1 & \bar{\nu}_1 r_1^2 & 0\end{pmatrix} M_{Tot,1}\vec{A}_N^{out} = 0 \tag{51}$$

This expression fails to produce $\sigma_r(r_1) = 0$ for the case of a plugged bore, that of $r_1 = 0$. However, it fortuitously reproduces the correct boundary condition for a plugged bore, that of:

$$u(r_1) = 0 \tag{52}$$

therefore Equation 51 can be used either for the open-bore or plugged bore case.

9.3 Constrained axial tension

The condition that F_z is constrained to a known value is, from Section 8:

$$\left(2\pi\left[\bar{E}_N\bar{\nu}_N\begin{pmatrix}r_{N+1}^2 & 1 & 0 & 0\end{pmatrix} - \bar{E}_1\bar{\nu}_1\begin{pmatrix}r_1^2 & 1 & 0 & 0\end{pmatrix} M_{Tot,1} + \sum_{i=2}^{N}(\bar{E}_{i-1}\bar{\nu}_{i-1} - \bar{E}_i\bar{\nu}_i)\begin{pmatrix}r_i^2 & 1 & 0 & 0\end{pmatrix} M_{Tot,i}\right] + \begin{pmatrix}0 & 0 & \langle\bar{E}A\rangle & -F_z\end{pmatrix}\right)\vec{A}_N^{out} = 0 \tag{53}$$

where $\langle\bar{E}A\rangle$ is defined in Equation 43

9.4 The boundary condition matrix

There is a reason that we have expressed each boundary condition and constraint as a row vector for an inner product. We can write the three constraints simultaneously as one matrix equation to

solve in Section 10:

$$M_{BC}\vec{A}_N^{out} = \begin{pmatrix} 0 \\ 0 \\ 0 \end{pmatrix} \tag{54}$$

where

$$M_{BC} = \begin{pmatrix} M_{BC,1} \\ M_{BC,2} \\ M_{BC,3} \end{pmatrix} \tag{55}$$

where $M_{BC,1}$ is the outer boundary condition inner product row vector

$$M_{BC,1} = \begin{pmatrix} (1+\bar{\nu}_N)r_{N+1}^2 & -1+\bar{\nu}_N & \bar{\nu}_N r_{N+1}^2 & 0 \end{pmatrix} \tag{56}$$

$M_{BC,2}$ is the inner boundary condition inner product row vector

$$M_{BC,2} = \begin{pmatrix} (1+\bar{\nu}_1)r_1^2 & -1+\bar{\nu}_1 & \bar{\nu}_1 r_1^2 & 0 \end{pmatrix} M_{Tot,1} \tag{57}$$

and $M_{BC,3}$ is the axial tension constraint inner product row vector

$$\begin{aligned} M_{BC,3} = \Bigg(& 2\pi \Big[\bar{E}_N \bar{\nu}_N \begin{pmatrix} r_{N+1}^2 & 1 & 0 & 0 \end{pmatrix} - \bar{E}_1 \bar{\nu}_1 \begin{pmatrix} r_1^2 & 1 & 0 & 0 \end{pmatrix} M_{Tot,1} \\ & + \sum_{i=2}^{N} (\bar{E}_{i-1}\bar{\nu}_{i-1} - \bar{E}_i \bar{\nu}_i) \begin{pmatrix} r_i^2 & 1 & 0 & 0 \end{pmatrix} M_{Tot,i} \Big] + \begin{pmatrix} 0 & 0 & \langle \bar{E}A \rangle & -F_z \end{pmatrix} \Bigg) \end{aligned} \tag{58}$$

10 The solution via matrix inversion

Because the M_{Int} and M_{Ext} matrices stack by matrix multiplication into the M_{Tot} matrices, it was convenient to include the column that multiplies the augmented fourth component (1) into the boundary condition matrix M_{BC}. However, for the purposes of solving Equation 54, it is convenient to now break the boundary condition matrix into the columns that multiply A, B, ϵ_z and the column that multiplies 1:

$$M_{BC}\vec{A}_N^{out} = M_{BC,1-3} \begin{pmatrix} A_N^{out} \\ B_N^{out} \\ \epsilon_z \end{pmatrix} + \begin{pmatrix} M_{BC,1,4} \\ M_{BC,2,4} \\ M_{BC,3,4} \end{pmatrix} = \begin{pmatrix} 0 \\ 0 \\ 0 \end{pmatrix} \tag{59}$$

where $M_{BC,1-3}$ is the matrix composed of only the first three columns of M_{BC}.

Thus the solution to this problem is:

$$\begin{pmatrix} A_N^{out} \\ B_N^{out} \\ \epsilon_z \end{pmatrix} = M_{BC,1-3}^{-1} \begin{pmatrix} -M_{BC,1,4} \\ -M_{BC,2,4} \\ -M_{BC,3,4} \end{pmatrix} \tag{60}$$

This is a 3×3 matrix inversion problem, which is easily susceptible to the standard numerical approaches such as Gaussian elimination. This is a very fast computation, appropriate for the inner loop of optimizers or parallel database approaches.

Notably, this algorithm is linear with the number of layers, with the computation of M_{Tot} taking the most time as N increases ($O(N)$ time). This is a favorable scaling compared to the inversion of a $2N \times 2N$ matrix (requiring $O(N^3)$ time as implemented in PROCESS via Gaussian elimination), which was the previous approach.

11 The model for transverse-isotropic materials

We will now generalize the model to transverse-isotropic materials, which have differing Young's Moduli and Poisson's Ratio in the axial vs transverse directions.

The the strains are computed from the normal stresses $\sigma_q \equiv \sigma_{qq}$ using the compliance form of Hooke's Law, which for a transverse-isotropic material is:

$$\epsilon_r = \frac{1}{E_\perp}\sigma_r - \frac{\nu_\perp}{E_\perp}\sigma_\theta - \frac{\nu_{z,\perp}}{E_z}\sigma_z \tag{61}$$

$$\epsilon_\theta = \frac{1}{E_\perp}\sigma_\theta - \frac{\nu_\perp}{E_\perp}\sigma_r - \frac{\nu_{z,\perp}}{E_z}\sigma_z \tag{62}$$

$$\epsilon_z = \frac{1}{E_z}\sigma_z - \frac{\nu_{\perp,z}}{E_\perp}\sigma_r - \frac{\nu_{\perp,z}}{E_\perp}\sigma_\theta \tag{63}$$

where $E_\perp$ is the Young's modulus in the transverse direction, E_z is the Young's modulus in the axial direction, $\nu_\perp$ is the Poisson's ratio between the two transverse directions, $\nu_{\perp,z}$ is the Poisson's ratio between the transverse and axial directions in that order, and $\nu_{z,\perp}$ is the Poisson's ratio between the axial and transverse directions in that order.

Because of the symmetry of the compliance tensor, $\nu_{z,\perp}$ and $\nu_{\perp,z}$ are not independent, such that

$$\frac{\nu_{\perp,z}}{E_\perp} = \frac{\nu_{z,\perp}}{E_z} \tag{64}$$

Anisotropic E, ν can come about when "uniform" layers are actually composed of fibers of differing material, long in the axial direction. The values of E, ν that result from this case are discussed in Section 13. Likely values of $E_z, E_\perp$ are the same as before in the tens to hundreds of gigapascals ($10^{10} - 10^{11}$ GPa). Values of $\nu_{z,\perp}$ are between 0 and 1/2, often around $\nu \sim 0.3$. The value of $\nu_{\perp,z}$ is computed from $\nu_{z,\perp}, E_\perp, E_z$ via Equation 64. Values of $\nu_\perp$ can be quite high, approaching 1 if axial stiffness is larger than transverse, being limited by the equation $\nu_\perp \leq 1 - \nu_{\perp,z}$. A likely value of $\nu_\perp$ might be 0.6 of this maximum.

These equations can be inverted into the stiffness form of Hooke's Law:

$$\sigma_r = \bar{E}_\perp(\epsilon_r + \bar{\nu}_\perp \epsilon_\theta + \bar{\nu}_{z,\perp}\epsilon_z) \tag{65}$$

$$\sigma_\theta = \bar{E}_\perp(\epsilon_\theta + \bar{\nu}_\perp \epsilon_r + \bar{\nu}_{z,\perp}\epsilon_z) \tag{66}$$

$$\sigma_z = \bar{E}_z(\epsilon_z + \bar{\nu}_{\perp,z}(\epsilon_r + \epsilon_\theta)) \tag{67}$$

Equations 65 - 67 replace Equations 7 - 9.

where $\bar{E}$ and $\bar{\nu}$ are the effective Young's modulus and Poisson's ratio holding *strain* rather than *stress* cross-terms constant [EDIT: Do these have names?]:

$$\bar{E}_z \equiv E_z \frac{1-\nu_\perp}{1-\nu_\perp - 2\nu_{\perp,z}\nu_{z,\perp}} \tag{68}$$

$$\bar{E}_\perp \equiv E_\perp \frac{1-\nu_{\perp,z}\nu_{z,\perp}}{(1-\nu_\perp - 2\nu_{\perp,z}\nu_{z,\perp})(1+\nu_\perp)}$$

$$\bar{\nu}_{\perp,z} \equiv \frac{\nu_{\perp,z}}{1-\nu_\perp} \tag{69}$$

$$\bar{\nu}_\perp \equiv \frac{\nu_\perp + \nu_{\perp,z}\nu_{z,\perp}}{1-\nu_{\perp,z}\nu_{z,\perp}}$$

$$\bar{\nu}_{z,\perp} \equiv \nu_{z,\perp}\frac{1+\nu_\perp}{1-\nu_{\perp,z}\nu_{z,\perp}}$$

Equations 68 - 69 replace Equations 10 - 11.

The body force balance equation is the same, but with $\bar{E}$ replaced with $\bar{E}_\perp$:

$$0 = \frac{1}{\bar{E}_\perp} f - \partial_r^2 u - \frac{1}{r}\partial_r u + \frac{1}{r^2}u \tag{70}$$

Equation 70 replaces Equation 13.

The radial and azimuthal stress are now:

$$\sigma_r(r) = \bar{E}_\perp[A(1+\bar{\nu}_\perp) - B(1-\bar{\nu}_\perp)\frac{1}{r^2} + \bar{\nu}_{z,\perp}\epsilon_z] \tag{71}$$

$$\sigma_\theta(r) = \bar{E}_\perp[A(1+\bar{\nu}_\perp) + B(1-\bar{\nu}_\perp)\frac{1}{r^2} + \bar{\nu}_{z,\perp}\epsilon_z] \tag{72}$$

Equations 71 and 72 replace Equations 16 and 17.

All transformation matrix elements are the same, but with with $\bar{E}$ replaced with $\bar{E}_\perp$ in all elements, with $\bar{\nu}$ replaced with $\bar{\nu}_\perp$ in elements $M_{i,1-2}$ and $\bar{\nu}_{z,\perp}$ in elements $M_{i,3}$:

$$\begin{pmatrix} A^{in} \\ B^{in} \\ \epsilon_z \\ 1 \end{pmatrix} = M_{Int} \begin{pmatrix} A^{out} \\ B^{out} \\ \epsilon_z \\ 1 \end{pmatrix} = \begin{bmatrix} 1 & 0 & 0 & -\frac{1}{2\bar{E}_\perp}\int_{r_{in}}^{r_{out}} dr \times f(r) \\ 0 & 1 & 0 & \frac{1}{2\bar{E}_\perp}\int_{r_{in}}^{r_{out}} dr \times r^2 f(r) \\ 0 & 0 & 1 & 0 \\ 0 & 0 & 0 & 1 \end{bmatrix} \begin{pmatrix} A^{out} \\ B^{out} \\ \epsilon_z \\ 1 \end{pmatrix} \tag{73}$$

$$\begin{pmatrix} A_{i-1}^{out} \\ B_{i-1}^{out} \\ \epsilon_z \\ 1 \end{pmatrix} = M_{Ext,i} \begin{pmatrix} A_i^{in} \\ B_i^{in} \\ \epsilon_z \\ 1 \end{pmatrix} = \begin{bmatrix} M_{1,1} & M_{1,2} & M_{1,3} & 0 \\ M_{2,1} & M_{2,2} & M_{2,3} & 0 \\ 0 & 0 & 1 & 0 \\ 0 & 0 & 0 & 1 \end{bmatrix} \begin{pmatrix} A_i^{in} \\ B_i^{in} \\ \epsilon_z \\ 1 \end{pmatrix} \tag{74}$$

$$M_{1,1} = \frac{1}{2}[\frac{\bar{E}_{\perp,i}}{\bar{E}_{\perp,i-1}}(1+\bar{\nu}_{\perp,i}) + 1 - \bar{\nu}_{\perp,i-1}] \tag{75}$$

$$M_{1,2} = \frac{1}{r_i^2}\frac{1}{2}[1 - \bar{\nu}_{\perp,i-1} - \frac{\bar{E}_{\perp,i}}{\bar{E}_{\perp,i-1}}(1-\bar{\nu}_{\perp,i})] \tag{76}$$

$$M_{1,3} = \frac{1}{2}[\frac{\bar{E}_{\perp,i}}{\bar{E}_{\perp,i-1}}\bar{\nu}_{z,\perp,i} - \bar{\nu}_{z,\perp,i-1}] \tag{77}$$

$$M_{2,1} = r_i^2(1 - M_{1,1}) \tag{78}$$

$$M_{2,2} = 1 - r_i^2 M_{1,2} \tag{79}$$

$$M_{2,3} = -r_i^2 M_{1,3} \tag{80}$$

Equation 73 replaces 23. Equations 74 - 80 replace Equations 30 - 36.

For the global boundary condition row vectors, the same $\bar{\nu}$ relationship holds:

$$M_{BC,1}\vec{A}_N^{out} = \begin{pmatrix} (1+\bar{\nu}_{\perp,N})r_{N+1}^2 & -1+\bar{\nu}_{\perp,N} & \bar{\nu}_{z,\perp,N}r_{N+1}^2 & 0 \end{pmatrix} \vec{A}_N^{out} = 0 \tag{81}$$

$$M_{BC,2}\vec{A}_N^{out} = \begin{pmatrix} (1+\bar{\nu}_{\perp,1})r_1^2 & -1+\bar{\nu}_{\perp,1} & \bar{\nu}_{z,\perp,1}r_1^2 & 0 \end{pmatrix} M_{Tot,1}\vec{A}_N^{out} = 0 \tag{82}$$

Equations 81 and 82 replace Equations 49 and 51.

For the axial force row vector, all $\bar{\nu}$ values are replaced with $\bar{\nu}_{\perp,z}$ and all $\bar{E}$ values are replaced with $\bar{E}_z$ values, including $\langle \bar{E}A \rangle \rightarrow \langle \bar{E}_z A \rangle$.

$$\begin{aligned} M_{BC,3} = \Bigg(& 2\pi \Big[\bar{E}_{z,N}\bar{\nu}_{\perp,z,N} \begin{pmatrix} r_{N+1}^2 & 1 & 0 & 0 \end{pmatrix} - \bar{E}_{z,1}\bar{\nu}_{\perp,z,1} \begin{pmatrix} r_1^2 & 1 & 0 & 0 \end{pmatrix} M_{Tot,1} \\ & + \sum_{i=2}^{N} (\bar{E}_{z,i-1}\bar{\nu}_{\perp,z,i-1} - \bar{E}_{z,i}\bar{\nu}_{\perp,z,i}) \begin{pmatrix} r_i^2 & 1 & 0 & 0 \end{pmatrix} M_{Tot,i} \Big] + \begin{pmatrix} 0 & 0 & \langle \bar{E}_z A \rangle & -F_z \end{pmatrix} \Bigg) \end{aligned} \tag{83}$$

Equation 83 replaces Equation 58.

12 Useful integrals of $f(r)$ for various forces

$f(r)$ is defined in Equation 12. It is the volumetric body force, such that $dF_r = f(r)dV$ where dV is a differential volume element.

$f(r)$ enters our problem in the form of two integrals, in Equations 18 and 19, respectively:

$$A(r) = A^{out} - \frac{1}{2\bar{E}} \int_r^{r_{out}} dr \times f(r)$$

$$B(r) = B^{out} + \frac{1}{2\bar{E}} \int_r^{r_{out}} dr \times r^2 f(r)$$

We will now discuss two useful functional forms of $f(r)$, the radially uniform case and the Lorentz force case.

12.1 The radially uniform case

This is a simple case, useful for evaluating the solution algorithm in a toy problem. This is what is implemented in MATLAB in Section 15.

This case is written:

$$f_i(r) = f_i \tag{84}$$

And the solutions to the equations are:

$$A_i(r) = A_i^{out} - \frac{1}{2\bar{E}_i} \int_r^{r_{i+1}} dr \times f_i(r) = A_i^{out} - \frac{1}{2\bar{E}_i} f_i(r_{i+1} - r) \tag{85}$$

$$B_i(r) = B_i^{out} + \frac{1}{2\bar{E}_i} \int_r^{r_{out}} dr \times r^2 f(r) = B_i^{out} + \frac{1}{6\bar{E}_i} f_i(r_{i+1}^3 - r^3) \tag{86}$$

Thus M_{Int} and Equation 23 become:

$$\begin{pmatrix} A_i^{in} \\ B_i^{in} \\ \epsilon_z \\ 1 \end{pmatrix} = M_{Int,i} \begin{pmatrix} A_i^{out} \\ B_i^{out} \\ \epsilon_z \\ 1 \end{pmatrix} = \begin{bmatrix} 1 & 0 & 0 & -\frac{1}{2\bar{E}_i} f_i(r_{i+1} - r_i) \\ 0 & 1 & 0 & \frac{1}{6\bar{E}_i} f_i(r_{i+1}^3 - r_i^3) \\ 0 & 0 & 1 & 0 \\ 0 & 0 & 0 & 1 \end{bmatrix} \begin{pmatrix} A_i^{out} \\ B_i^{out} \\ \epsilon_z \\ 1 \end{pmatrix}$$

12.2 The Lorentz force case

This section evaluates the case that the force density $f(r)$ results from a current density j_i in the $\hat{z}$ axial direction, uniform within each layer i. $f(r)$ is computed using the Lorentz force, $f_r = j_z B_\theta$, where B_θ is found using Ampere's law.

Computing this, we find that

$$f_i(r) = \frac{\mu_0}{2\pi}\left[j_i(\sum_{p<i}\Delta I_p)\frac{1}{r} - j_i^2\pi r_i^2\frac{1}{r} + j_i^2\pi r\right] \tag{87}$$

where μ_0 is the permeability of free space, $\mu_0 \equiv 4\pi \times 10^{-7}$ H/m, and ΔI_p is the current carried by layer p:

$$\Delta I_p = \int_{r_p}^{r_{p+1}} dr \times 2\pi r j(r) = j_p\pi(r_{p+1}^2 - r_p^2) \tag{88}$$

The necessary integrals are also analytically solvable:

$$\int_r^{r_{i+1}} dr \times f_i(r) = \frac{\mu_0}{2\pi}\left[\left(j_i(\sum_{p<i}\Delta I_p) - j_i^2\pi r_i^2\right)\ln\frac{r_{i+1}}{r} + \frac{1}{2}j_i^2\pi(r_{i+1}^2 - r^2)\right] \tag{89}$$

$$\int_r^{r_{i+1}} dr \times r^2 f_i(r) = \frac{\mu_0}{2\pi}\left[\left(j_i(\sum_{p<i}\Delta I_p) - j_i^2\pi r_i^2\right)\frac{1}{2}(r_{i+1}^2 - r^2) + \frac{1}{4}j_i^2\pi(r_{i+1}^4 - r^4)\right] \tag{90}$$

Recall that the quantities to plug into Equation 23 to obtain $M_{Int,i}$ are these integrals evaluated at $r = r_i$. They have been left in their fully general form so that $A(r), B(r)$ may be computed, allowing computation of stresses, strains, and displacement at all r, not just the boundaries.

13 Property "smearing"

If two member are in parallel, that is they both connect to terminals at which force is applied, the effective Young's modulus of the composite member can be computed from the assumption that both members have the same strain. The result is an areal average of the individual Young's moduli:

$$E_{parallel} = \frac{\sum_i A_i E_i}{\sum_i A_i} = \langle E \rangle \tag{91}$$

where A_i is the cross-section area of member i.

The Poisson's ratios add in the same way:

$$\nu_{parallel} = \frac{\sum_i A_i \nu_i}{\sum_i A_i} = \langle \nu \rangle \tag{92}$$

If two members are in series, that is one member connects a terminal to the other member, which connects to a terminal, the effective Young's modulus of the composite member can be computed from the assumption that both members have the same stress. The result is an inverse average of the weighted average of the individual Young's moduli:

$$E_{series} = \frac{\sum_i L_i}{\sum_i L_i/E_i} = \frac{1}{\langle 1/E \rangle} \tag{93}$$

where L_i is the length of member i.

The Poisson's ratios add in a similar way, but weighted by the inverse Young's modulus:

$$\nu_{series} = \frac{\sum_i L_i \nu_i / E_i}{\sum_i L_i / E_i} \tag{94}$$

If the layers are made of bundles of axial fibers, or bundles of axial fibers embedded in a bulk matrix, then properties in the axial direction will sum in the parallel way, and properties in the transverse direction will sum in the series way. Furthermore, if the fibers are small and randomly distributed (not in a regular grid), the various dimension-averages A_i, L_i can just be assumed to take the value of the volume fraction f_V of that material:

$$E_{parallel} \to E_z$$

$$\nu_{parallel} \to \nu_z$$

$$A_i \to f_{V,i}$$

$$E_{series} \to E_\perp$$

$$\nu_{series} \to \nu_\perp$$

$$L_i \to f_{V,i}$$

In the PROCESS code as implemented, the above assumption (small fibers, randomly distributed, volume-averaged materials) is *not* assumed. Rather, a perfect rectangular grid is used, and series and parallel sums are nested to produce bulk materials properties. The relative applicabilites of these competing models is not settled.

14 If the innermost layers do not contribute to the axial force

For many tokamaks, the TF coil is positioned radially outward of another structure, the Central Solenoid (CS). For "bucked and wedged" tokamaks,[17] the inner layer of the TF coil is in contact with the outer layer of the Central Solenoid (CS), but there is a friction-free layer between them, which allows the CS not to expand with the TF coil when axial force F_z is applied to the latter. This invalidates the assumption that ϵ_z is constant. Outward of some radius, as before, ϵ_z is set by the condition that the axial stress must integrate to F_z. But inward of that radius, ϵ_z is set by the condition that there is no axial force.

Suppose that the innermost layer which contributes to F_z is layer i_F. Layers with $i < i_F$ do not contribute to F_z, and layers with $i \geq i_F$ do contribute to F_z.

To adapt the model to this condition, all of the matrices must change. Most notably the "external transformation matrix" M_{Ext} discussed in Section 6, and the axial tension row of the boundary condition matrix, $M_{BC,3}$, discussed in Sections 8 and 9.

Because there are now *two* unknown axial strains, we must increase the dimension of the solution vector. This section uses the following convention:

$$\vec{A}_i^j = \begin{pmatrix} A_i^j \\ B_i^j \\ \epsilon_{z,out} \\ 1 \\ \epsilon_{z,in} \end{pmatrix} \tag{95}$$

where $\epsilon_{z,out}$ is the axial stress of the outer layers which contribute to F_z (layers with $i \geq i_F$) and $\epsilon_{z,in}$ is the axial stress of the inner layers which do not contribute to F_z (layers with $i < i_F$). $\epsilon_{z,in}$ was added in position 5 in the vector, rather than position 4, so as to keep the matrices as similar as possible.

To M_{Int}, the only change is the addition to another column and row. This equation replaces Equation 23:

$$\begin{pmatrix} A^{in} \\ B^{in} \\ \epsilon_{z,out} \\ 1 \\ \epsilon_{z,in} \end{pmatrix} = M_{Int} \begin{pmatrix} A^{out} \\ B^{out} \\ \epsilon_{z,out} \\ 1 \\ \epsilon_{z,in} \end{pmatrix} = \begin{bmatrix} 1 & 0 & 0 & -\frac{1}{2\bar{E}} \int_{r_{in}}^{r_{out}} dr \times f(r) & 0 \\ 0 & 1 & 0 & \frac{1}{2\bar{E}} \int_{r_{in}}^{r_{out}} dr \times r^2 f(r) & 0 \\ 0 & 0 & 1 & 0 & 0 \\ 0 & 0 & 0 & 1 & 0 \\ 0 & 0 & 0 & 0 & 1 \end{bmatrix} \begin{pmatrix} A^{out} \\ B^{out} \\ \epsilon_{z,out} \\ 1 \\ \epsilon_{z,in} \end{pmatrix} \tag{96}$$

To M_{Ext}, the changes are more serious:

$$\begin{pmatrix} A_{i-1}^{out} \\ B_{i-1}^{out} \\ \epsilon_{z,out} \\ 1 \\ \epsilon_{z,in} \end{pmatrix} = M_{Ext,i} \begin{pmatrix} A_i^{in} \\ B_i^{in} \\ \epsilon_{z,out} \\ 1 \\ \epsilon_{z,in} \end{pmatrix} = \begin{bmatrix} M_{1,1} & M_{1,2} & M_{1,3} & 0 & M_{1,5} \\ M_{2,1} & M_{2,2} & M_{2,3} & 0 & M_{2,5} \\ 0 & 0 & 1 & 0 & 0 \\ 0 & 0 & 0 & 1 & 0 \\ 0 & 0 & 0 & 0 & 1 \end{bmatrix} \begin{pmatrix} A_i^{in} \\ B_i^{in} \\ \epsilon_{z,out} \\ 1 \\ \epsilon_{z,in} \end{pmatrix} \tag{97}$$

$M_{1,1}, M_{1,2}, M_{2,1}, M_{2,2}$ stay the same. $M_{1,3}, M_{1,5}, M_{2,3}, M_{2,5}$ are different, and have different form depending on the relative values of i, i_F:

$$M_{1,3} = \begin{cases} \frac{1}{2}[\frac{\bar{E}_i}{\bar{E}_{i-1}} \bar{\nu}_i - \bar{\nu}_{i-1}] & (i > i_F) \\ \frac{1}{2}[\frac{\bar{E}_i}{\bar{E}_{i-1}} \bar{\nu}_i] & (i = i_F) \\ 0 & (i < i_F) \end{cases} \tag{98}$$

$$M_{1,5} = \begin{cases} 0 & (i > i_F) \\ \frac{1}{2}[-\bar{\nu}_{i-1}] & (i = i_F) \\ \frac{1}{2}[\frac{\bar{E}_i}{\bar{E}_{i-1}} \bar{\nu}_i - \bar{\nu}_{i-1}] & (i < i_F) \end{cases}$$

$$M_{2,3} = -r_i^2 M_{1,3}$$

$$M_{2,5} = -r_i^2 M_{1,5}$$

The outer boundary condition, $M_{BC,1}$ in Section 9, needs a minor alteration.

$$M_{BC,1} = \begin{pmatrix} (1+\bar{\nu}_N)r_{N+1}^2 & -1+\bar{\nu}_N & \bar{\nu}_N r_{N+1}^2 & 0 & 0 \end{pmatrix} \tag{99}$$

The inner boundary condition, $M_{BC,2}$ in Section 9, also needs a minor alteration which depends on whether $i_F > 1$, that is whether the axial force decoupling is being actively used.

$$M_{BC,2} = \begin{cases} \begin{pmatrix} (1+\bar{\nu}_1)r_1^2 & -1+\bar{\nu}_1 & 0 & 0 & \bar{\nu}_1 r_1^2 \end{pmatrix} M_{Tot,1} & (i_F > 1) \\ \begin{pmatrix} (1+\bar{\nu}_1)r_1^2 & -1+\bar{\nu}_1 & \bar{\nu}_1 r_1^2 & 0 & 0 \end{pmatrix} M_{Tot,1} & (i_F = 1) \end{cases} \tag{100}$$

The axial force inner product, which is expressed as $F_{z,\bar{\nu}}$ in Section 8 and $M_{BC,3}$ in Section 9, must now become two inner products. This equation replaces Equation 58:

$$\begin{aligned} M_{BC,3} = \Bigg(& 2\pi \Big[\bar{E}_N \bar{\nu}_N \begin{pmatrix} r_{N+1}^2 & 1 & 0 & 0 & 0 \end{pmatrix} - \bar{E}_{i_F} \bar{\nu}_{i_F} \begin{pmatrix} r_{i_F}^2 & 1 & 0 & 0 & 0 \end{pmatrix} M_{Tot,i_F} \\ & + \sum_{i=i_F+1}^{N} \left(\bar{E}_{i-1}\bar{\nu}_{i-1} - \bar{E}_i \bar{\nu}_i \right) \begin{pmatrix} r_i^2 & 1 & 0 & 0 & 0 \end{pmatrix} M_{Tot,i} \Big] + \begin{pmatrix} 0 & 0 & \langle \bar{E}A \rangle_{out} & -F_z & 0 \end{pmatrix} \Bigg) \end{aligned} \tag{101}$$

where $\langle \bar{E}A \rangle_{out}$ is

$$\langle \bar{E}A \rangle_{out} = \pi \sum_{i=i_F}^{N} \bar{E}_i (r_{i+1}^2 - r_i^2) \tag{102}$$

We now need another boundary condition, $M_{BC,4}$, which enforces that there is zero axial force on the inner subset, layers for which $i < i_F$:

$$\begin{aligned} M_{BC,4} = \Bigg(& 2\pi \Big[\bar{E}_{i_F-1} \bar{\nu}_{i_F-1} \begin{pmatrix} r_{i_F}^2 & 1 & 0 & 0 & 0 \end{pmatrix} M_{Tot,i_F} - \bar{E}_1 \bar{\nu}_1 \begin{pmatrix} r_1^2 & 1 & 0 & 0 & 0 \end{pmatrix} M_{Tot,1} \\ & + \sum_{i=2}^{i_F-1} \left(\bar{E}_{i-1}\bar{\nu}_{i-1} - \bar{E}_i \bar{\nu}_i \right) \begin{pmatrix} r_i^2 & 1 & 0 & 0 & 0 \end{pmatrix} M_{Tot,i} \Big] + \begin{pmatrix} 0 & 0 & 0 & 0 & \langle \bar{E}A \rangle_{in} \end{pmatrix} \Bigg) \end{aligned} \tag{103}$$

where $\langle \bar{E}A \rangle_{in}$ is

$$\langle \bar{E}A \rangle_{in} = \pi \sum_{i=1}^{i_F-1} \bar{E}_i (r_{i+1}^2 - r_i^2) \tag{104}$$

The matrix inversion / Gaussian elimination, Equations 59 and 60 in Section 10 must also change:

$$M_{BC} \vec{A}_N^{out} = M_{BC,1-3,5} \begin{pmatrix} A_N^{out} \\ B_N^{out} \\ \epsilon_{z,out} \\ \epsilon_{z,in} \end{pmatrix} + \begin{pmatrix} M_{BC,1,4} \\ M_{BC,2,4} \\ M_{BC,3,4} \\ M_{BC,4,4} \end{pmatrix} = \begin{pmatrix} 0 \\ 0 \\ 0 \\ 0 \end{pmatrix} \tag{105}$$

where $M_{BC,1-3,4}$ is the matrix composed of columns 1, 2, 3, and 5 of M_{BC}.

Thus the solution to this problem is:

$$\begin{pmatrix} A_N^{out} \\ B_N^{out} \\ \epsilon_{z,out} \\ \epsilon_{z,in} \end{pmatrix} = M_{BC,1-3,4}^{-1} \begin{pmatrix} -M_{BC,1,4} \\ -M_{BC,2,4} \\ -M_{BC,3,4} \\ -M_{BC,4,4} \end{pmatrix} \tag{106}$$

15 A MATLAB implementation of this model

```
% Charles Swanson, cswanson@pppl.gov
% 2022/02/14

% This MATLAB script is the companion to the extended plane strain paper. It
% assumes N uniform layers with random thicknesses, materials properties, and
% Lorentz body forces. Materials properties are transverse-isotropic. It assumes
% a random, known axial tension. It calcualtes the Lame parameter solution
% vector, the axial strains, the radial displacement as a function of
% radius, the radial and azimuthal strain as a function of radius, and the
% radial, azimuthal, and axial stress as a function of radius. Includes
% frictional decoupling of an inner set of layers; only the outer layers
% contribute to the axial force.

close all;clear all;

%% Set up input parameters

% Which body force model to use. % True: Lorentz. False: Uniform.
boolLorentz = true; % Lorentz force

% Innermost layer which still contributes to Fz
%innerFzLayer = 1; % Uniform strain, no decoupled layer
innerFzLayer = 5; % This layer and outward contribute to Fz

% Number of layers
N = 10;

% Layer thicknesses. dr(i+1) is thickness of layer i.
% dr(1) is innermost point. dr(1)=0 corresponds to plugged bore.
dr     = rand(1,N+1);
%dr(1)  = 0; % Plugged

% Force in the Z direction
```

```
Fz = 100e9*rand;
if boolLorentz
  % Layer currents for body force calculation
  dI = 100e6*rand(1,N);
else
  % uniform radial body force densities;
  f  = 100e6*(1-2*rand(1,N));
end

% Young's moduli and Poisson's ratios
Ez   = 200e9*rand(1,N); % Axial Young's modulus
Et   = 200e9*rand(1,N); % Transverse Young's modulus
nut  = 0.5*rand(1,N); % Transverse-transverse Poisson's ratio
nutz = 0.5*rand(1,N); % Transverse-axial Poisson's ratio
nuzt = 0.5*rand(1,N); % Axial-transverse Poisson's ratio

%% Set up the geometry and materials properties:

% Inter-layer spacing, r(1) is innermost surface, r(N+1) is outermost surface
% r(j) separates layer j-1 from layer j
% dr(1) = 0 corresponds to plugged bore
sumMat = 1:(N+1);
sumMat = sumMat>=sumMat';
r      = sum(sumMat.*dr',1);

%% SECTION 3:
% With transverse-isotropic materials properties from Section 12

% nutz set by symmetry of compliance tensor
nutz    = nuzt .* Et ./ Ez;
% Effective Young's moduli and Poisson's ratios in stiffness form
EzBar   = Ez .* (1-nut) ./ (1-nut-2*nutz.*nuzt);
EtBar   = Et .* (1-nutz.*nuzt) ./ (1-nut-2*nutz.*nuzt) ./ (1+nut);
nutBar  = (nut+nutz.*nuzt) ./ (1-nutz.*nuzt);
nutzBar = nutz ./ (1-nut);
nuztBar = nuzt .* (1+nut) ./ (1-nutz.*nuzt);

%% SECTION 13:
% General body force integrals

if boolLorentz
  % Permeability of free space
  mu0    = 4*pi*1e-7;
  % Current enclosed within the inner radius of each layer
  sumMat = 1:N;
  sumMat = sumMat>sumMat';
```

```
  IEnc   = sum(sumMat.*dI',1);
  % Current density of each layer
  j      = dI./pi./(r(2:end).^2-r(1:(end-1)).^2);
  % Factors that multiply r linearly and reciprocally in force density
  fLinFac = mu0/2 * j.^2;
  fRecFac = mu0/2 * (j.*IEnc/pi - j.^2.*r(1:N).^2);

  % Lorentz body force f
  % Body force
  fBody = @(rArg,layer) fLinFac(layer).*rArg + fRecFac(layer)./rArg;
  % A integral, integral of f: (including correction for if r(1)==0)
  fIntA = @(rArg,layer) 1/2*fLinFac(layer).*(r(layer+1).^2-rArg.^2) + ...
    fRecFac(layer).*log(r(layer+1)./(rArg+(fRecFac(layer)==0)));
  % B integral, integral of fr^2:
  fIntB = @(rArg,layer) 1/4*fLinFac(layer).*(r(layer+1).^4-rArg.^4) + ...
    1/2*fRecFac(layer).*(r(layer+1).^2-rArg.^2);

else
  % Uniform body force f
  % Body force
  fBody = @(rArg,layer) f(layer);
  % A integral, integral of f:
  fIntA = @(rArg,layer) f(layer).*(r(layer+1)-rArg);
  % B integral, integral of fr^2:
  fIntB = @(rArg,layer) 1/3*f(layer)*(r(layer+1).^3-rArg.^3);

end

%% SECTION 5:
% With transverse-isotropic materials properties from Section 12
% With axial decoupling of inner layers from Section 15

% Generate each MInt(:,:,j), transfer matrix within one layer, such that
% (AIn(j);BIn(j);epsZOut;1;epsZIn) = MInt(:,:,j)*(AOut(j);BOut(j);epsZOut;1;epsZIn)
MInt = zeros(5,5,N);
for layer = 1:N
  MInt(1,1,layer) = 1;
  MInt(1,4,layer) = -1/2/EtBar(layer)*fIntA(r(layer),layer);
  MInt(2,2,layer) = 1;
  MInt(2,4,layer) = 1/2/EtBar(layer)*fIntB(r(layer),layer);
  MInt(3,3,layer) = 1;
  MInt(4,4,layer) = 1;
  MInt(5,5,layer) = 1;
end

%% SECTION 6:
```

```
% With transverse-isotropic materials properties from Section 12
% With axial decoupling of inner layers from Section 15

% Generate each MExt(:,:,j), transfer matrix for layer boundaries, such that
% (AOut(j-1);BOut(j-1);epsZOut,epsZIn;1) = MExt(:,:,j)*(AIn(j);BIn(j);epsZOut,epsZIn;1)
MExt = zeros(5,5,N);
for layer = 2:N
  EFac = EtBar(layer)/EtBar(layer-1);
  MExt(1,1,layer) = 1/2*(EFac*(1+nutBar(layer))+1-nutBar(layer-1));
  MExt(1,2,layer) = 1/2/r(layer)^2*(1-nutBar(layer-1)-EFac*(1-nutBar(layer)));
  if layer==innerFzLayer
    MExt(1,3,layer) = 1/2*EFac*nuztBar(layer);
    MExt(1,5,layer) = 1/2*(-nuztBar(layer-1));
  elseif layer<innerFzLayer
    MExt(1,3,layer) = 0;
    MExt(1,5,layer) = 1/2*(EFac*nuztBar(layer)-nuztBar(layer-1));
  elseif layer>innerFzLayer
    MExt(1,3,layer) = 1/2*(EFac*nuztBar(layer)-nuztBar(layer-1));
    MExt(1,5,layer) = 0;
  end
  MExt(2,1,layer) = r(layer)^2*(1-MExt(1,1,layer));
  MExt(2,2,layer) = (1-r(layer)^2*MExt(1,2,layer));
  MExt(2,3,layer) = -r(layer)^2*MExt(1,3,layer);
  MExt(2,5,layer) = -r(layer)^2*MExt(1,5,layer);
  MExt(3,3,layer) = 1;
  MExt(4,4,layer) = 1;
  MExt(5,5,layer) = 1;
end

%% SECTION 7
% With axial decoupling of inner layers from Section 15

% Generate a total MTot matrix for ease of relating global boundaries, relating
% AIn(j),BIn(j) to AOut(N),BOut(N)
MTot = zeros(5,5,N);
MTot(:,:,N) = (1:5)==(1:5)';
MTot(:,:,N) = MInt(:,:,N)*MTot(:,:,N);
for layer = (N-1):-1:1
  MTot(:,:,layer) = MInt(:,:,layer)*MExt(:,:,layer+1)*MTot(:,:,layer+1);
end

%% SECTION 8
% With transverse-isotropic materials properties from Section 12
% With axial decoupling of inner layers from Section 15

% Effective axial stiffness times cross sectional area
```

```
EBarAvgArea    = pi*EzBar.*(r(2:end).^2-r(1:N).^2);
EBarAvgAreaOut = sum(EBarAvgArea(innerFzLayer:end));
EBarAvgAreaIn  = sum(EBarAvgArea(1:(innerFzLayer-1)));

% The Fz evalution row of the matrix
FzRowOut = 2*pi*(EzBar(N)*nutzBar(N)*[r(end).^2 1 0 0 0] - ...
  EzBar(innerFzLayer)*nutzBar(innerFzLayer)*[r(innerFzLayer).^2 1 0 0 0]*MTot(:,:,innerFzLayer));
for layer = (innerFzLayer+1):N
  FzRowOut = FzRowOut + 2*pi*(EzBar(layer-1)*nutzBar(layer-1) - ...
    EzBar(layer)*nutzBar(layer))*([r(layer).^2 1 0 0 0]*MTot(:,:,layer));
end
% Include the effect of axial stiffness
FzRowOut(3) = FzRowOut(3) + EBarAvgAreaOut;

if innerFzLayer>1
  % The Fz evalution row of the matrix
  FzRowIn = 2*pi*(EzBar(innerFzLayer-1)*nutzBar(innerFzLayer-1)* ...
    [r(innerFzLayer).^2 1 0 0 0]*MTot(:,:,innerFzLayer) - ...
    EzBar(1)*nutzBar(1)*[r(1).^2 1 0 0 0]*MTot(:,:,1));
  for layer = 2:(innerFzLayer-1)
    FzRowIn = FzRowIn + 2*pi*(EzBar(layer-1)*nutzBar(layer-1) - ...
      EzBar(layer)*nutzBar(layer))*([r(layer).^2 1 0 0 0]*MTot(:,:,layer));
  end
  % Include the effect of axial stiffness
  FzRowIn(5) = FzRowIn(5) + EBarAvgAreaIn;
else
  FzRowIn = [0 0 0 0 1];
end

%% SECTION 9
% With transverse-isotropic materials properties from Section 12
% With axial decoupling of inner layers from Section 15

% The boundary condition matrix, MBC*[AOut(N);BOut(N);epsZOut;1epsZIn] = 0
MBC = [(1+nutBar(end))*r(end)^2 -1+nutBar(end) nuztBar(end)*r(end)^2 0 0;
  [(1+nutBar(1))*r(1).^2 -1+nutBar(1) [(innerFzLayer<=1) 0 (innerFzLayer>1)].* ...
    nuztBar(1)*r(1)^2]*MTot(:,:,1);
  FzRowOut-[0 0 0 Fz 0]
  FzRowIn];

%% SECTION 10
% With transverse-isotropic materials properties from Section 12
% With axial decoupling of inner layers from Section 15

% The solution vector via matrix inversion
MBCSolvEff = MBC(:,[1:3 5]);
```

```
RHSVec     = [-MBC(1,4);-MBC(2,4);-MBC(3,4);-MBC(4,4)];
AVecSolution = MBCSolvEff\RHSVec;
AVecSolution = [AVecSolution(1:3);1;AVecSolution(4)];

%% PLOT OUTPUTS

% Vectors of Lame parameters
AOut = zeros(1,N);
AIn = zeros(1,N);
BOut = zeros(1,N);
BIn = zeros(1,N);

% Set outward solution vector
AOut(N) = AVecSolution(1);
BOut(N) = AVecSolution(2);
epsZOut = AVecSolution(3);
epsZIn  = AVecSolution(5);

% Set each A(j), B(j)
for layer = 2:N
  AVecLayer = MTot(:,:,layer)*AVecSolution;
  AIn(layer) = AVecLayer(1);
  BIn(layer) = AVecLayer(2);

  AVecLayer = MExt(:,:,layer)*AVecLayer;
  AOut(layer-1) = AVecLayer(1);
  BOut(layer-1) = AVecLayer(2);
end
AVecLayer = MTot(:,:,1)*AVecSolution;
AIn(1)    = AVecLayer(1);
BIn(1)    = AVecLayer(2);

% Plotting domain
drPlot = 1e-3;
rPlot  = r(1):drPlot:r(N+1);
rPlot  = [rPlot r(N+1)];
inds   = 1:numel(rPlot);

% Populate each each layer's plotting functions
for layer = 1:N
  boolRange = (rPlot<=r(layer+1)).*(rPlot>=r(layer));
  inRange = inds(boolRange==1);

  % Local values of A, B coefficients
  APlot(inRange) = AOut(layer) - 1/2/EtBar(layer)*fIntA(rPlot(inRange),layer);
  BPlot(inRange) = BOut(layer) + 1/2/EtBar(layer)*fIntB(rPlot(inRange),layer);
```

```
  % Local values of materials properties
  EzBarPlot(inRange)   = EzBar(layer);
  EtBarPlot(inRange)   = EtBar(layer);
  nutBarPlot(inRange)  = nutBar(layer);
  nutzBarPlot(inRange) = nutzBar(layer);
  nuztBarPlot(inRange) = nuztBar(layer);

  EzPlot(inRange)   = Ez(layer);
  EtPlot(inRange)   = Et(layer);
  nutPlot(inRange)  = nut(layer);
  nutzPlot(inRange) = nutz(layer);
  nuztPlot(inRange) = nuzt(layer);

  epsZPlot(inRange) = ones(size(inRange)).*((layer>=innerFzLayer)*epsZOut + ...
    (layer<innerFzLayer)*epsZIn);
end

% Displacement
uPlot = APlot.*rPlot + BPlot./rPlot;

% Strains
epsRPlot     = APlot - BPlot./rPlot.^2;
epsThetaPlot = APlot + BPlot./rPlot.^2;

% Stresses
sigRPlot     = EtBarPlot.*((1+nutBarPlot).*APlot - (1-nutBarPlot).*BPlot./rPlot.^2 + ...
  nuztBarPlot.*epsZPlot);
sigThetaPlot = EtBarPlot.*((1+nutBarPlot).*APlot + (1-nutBarPlot).*BPlot./rPlot.^2 + ...
  nuztBarPlot.*epsZPlot);
sigZPlot     = EzBarPlot.*(epsZPlot + nutzBarPlot.*(epsRPlot + epsThetaPlot));
```

16 References

References

[1] F. J. Mangiarotti, J. Goh, M. Takayasu, L. Bromberg, J. V. Minervini, and D. Whyte, "Demountable Toroidal Field Magnets for Use in a Compact Modular Fusion Reactor," *Journal of Physics: Conference Series*, vol. 507, p. 032030, May 2014. Publisher: IOP Publishing.

[2] M. Kovari, R. Kemp, H. Lux, P. Knight, J. Morris, and D. J. Ward, ""PROCESS": A systems code for fusion power plants—Part 1: Physics," *Fusion Engineering and Design*, vol. 89,

pp. 3054–3069, Dec. 2014.

[3] M. Kovari, F. Fox, C. Harrington, R. Kembleton, P. Knight, H. Lux, and J. Morris, ""PROCESS": A systems code for fusion power plants – Part 2: Engineering," *Fusion Engineering and Design*, vol. 104, pp. 9–20, Mar. 2016.

[4] A. E. Costley, J. Hugill, and P. F. Buxton, "On the power and size of tokamak fusion pilot plants and reactors," *Nuclear Fusion*, vol. 55, p. 033001, Jan. 2015. Publisher: IOP Publishing.

[5] A. E. Costley, "Towards a compact spherical tokamak fusion pilot plant," *Philosophical Transactions of the Royal Society A: Mathematical, Physical and Engineering Sciences*, vol. 377, p. 20170439, Mar. 2019. Publisher: Royal Society.

[6] R. D. Stambaugh, V. S. Chan, A. M. Garofalo, M. Sawan, D. A. Humphreys, L. L. Lao, J. A. Leuer, T. W. Petrie, R. Prater, P. B. Snyder, J. P. Smith, and C. P. C. Wong, "Fusion Nuclear Science Facility Candidates," *Fusion Science and Technology*, vol. 59, pp. 279–307, Feb. 2011. Publisher: Taylor & Francis _eprint: https://doi.org/10.13182/FST59-279.

[7] R. J. Buttery, J. M. Park, J. T. McClenaghan, D. Weisberg, J. Canik, J. Ferron, A. Garofalo, C. T. Holcomb, J. Leuer, and P. B. Snyder, "The advanced tokamak path to a compact net electric fusion pilot plant," *Nucl. Fusion*, p. 19, 2021.

[8] C. E. Kessel, D. B. Batchelor, P. T. Bonoli, M. E. Rensink, T. D. Rognlien, P. Snyder, G. M. Wallace, and S. J. Wukitch, "Core plasma physics basis and its impacts on the FNSF," *Fusion Engineering and Design*, vol. 135, pp. 356–369, Oct. 2018.

[9] C. Kessel and M. Tillack, "FESS Conference Call," Apr. 2021.

[10] J. P. Freidberg, F. J. Mangiarotti, and J. Minervini, "Designing a tokamak fusion reactor—How does plasma physics fit in?," *Physics of Plasmas*, vol. 22, p. 070901, July 2015. Publisher: American Institute of Physics.

[11] D. J. Segal, A. J. Cerfon, and J. P. Freidberg, "Steady state versus pulsed tokamak reactors," *Nuclear Fusion*, Jan. 2021. Publisher: IOP Publishing.

[12] djsegal, "djsegal/FusionSystems.jl," Nov. 2020. `https://github.com/djsegal/FusionSystems.jl`.

[13] F. C. Moon, "The virial theorem and scaling laws for superconducting magnet systems," *Journal of Applied Physics*, vol. 53, pp. 9112–9121, Dec. 1982. Publisher: American Institute of Physics.

[14] A.-D. Cheng, J. Rencis, and Y. Abousleiman, "Generalized Plane Strain Elasticity Problems," *WIT Transactions on Modelling and Simulation*, vol. 10, pp. 167–174, July 1995.

[15] S. Kahn, "Derivation of multilayer generalized plane strain modelling for inboard mid-plane stress calculations," document uploaded to Gitlab issue tracker, Culham Centre for Fusion Energy, Jan. 2020. Not public (requires UKAEA network access) `https://git.ccfe.ac.uk/process/process/-/issues/991`.

[16] S. Kahn, "Toroidal Field Coils, PROCESS Documentation." Not public (requires UKAEA network access) `http://process.gitpages.ccfe.ac.uk/process/eng-models/tf-coil/`.

[17] P. Titus, "Structural Design of High Field Tokamaks," Tech. Rep. PSFC/JA-03-9, Plasma Science and Fusion Center Massachusetts Institute of Technology, Cambridge MA 02139 USA, June 2003. Accepted: 2015-02-10T20:13:14Z Publisher: MIT Plasma Science and Fusion Center.